Master/slave based optical coherence tomography for *in-vivo*, real-time, long axial imaging range of the anterior segment

Adrian Bradu*[a], Sylvain Rivet[b], and Adrian Podoleanu[a]
[a]Applied Optics Group, School of Physical Sciences, University of Kent, CT2 7NH Canterbury, UK
[b]Université de Bretagne Occidentale, EA 938 Lab. De Spectrométrie et Optique Laser, Brest, France

ABSTRACT

In this report, we demonstrate that in a coherence revival (CR) based swept source optical coherence tomography (SS-OCT) set-up, real-time cross-sectional long-range images can be produced via the Master Slave (MS) method. The total tolerance of the MS method to nonlinear tuning, to dispersion in the interferometer and to dispersion due to the laser cavity, makes the MS ideally suited to the practice of coherence revival. In addition, enhanced versatility is allowed by the MS method in displaying shorter axial range images than that determined by the digital sampling of the data. This brings an immediate improvement in the speed of displaying cross-sectional images at high rates without the need of extra hardware such as graphics processing units or field programmable gate arrays. The long axial range of the coherence revival regime is proven with images of the anterior segment of healthy human eye.

1. INTRODUCTION

Swept source optical coherence tomography imaging instruments can be used to produce cross-sectional OCT images with high speed, sensitivity and axial ranges longer than those provided by camera based ones. However, there are applications that could benefit from an even more extended imaging range, than that ensured by the current SS technology.

Due to the finite coherence length of the lasers used, the axial imaging range is still limited. An exception from this makes the new vertical-cavity surface-emitting lasers VCSEL and akinetic sources, available at around 1300 and 1550 nm. For shorter wavelengths, around 1050 nm, there are no SS sources capable of providing high resolution extended (cm) axial ranges.

A solution to increase the axial range in SS-OCT is the use of the coherence revival exhibited by some external cavity tunable laser (ECTL) swept sources [1-6]. The CR method is easy to implement, as only the optical path difference between the two arms of the interferometer needs to be altered. However, there are some penalties in implementing the CR method via the conventional Fast Fourier Transform (FFT) based method:

(i) The k-clock equipping the ECTL swept source becomes unusable for correct data digitization.

(ii) Intensive dispersion compensation is required. While for compensating for the dispersion in the interferometer both hardware optical methods and software methods can be implemented, to compensate for the dispersion due to the laser cavity, only software solutions can be used.

In the present report, based on reference [6], we demonstrate, as an alternative to the FFT method, the utilization of the recently introduced master/slave method in combination with the coherence revival technique, which eliminates the drawbacks specified above and allows real-time production of cross-sectional images.

2. METHODS

The procedures of producing B-scans, using the FFT and MS based OCT methods are completely different [7-11]. As illustrated in Fig. 1, although both techniques require a “calibration” step, before data acquisition, the FFT method entails 3 operations, after data being acquired, which can only be executed sequentially whilst the MS entails a single operation.

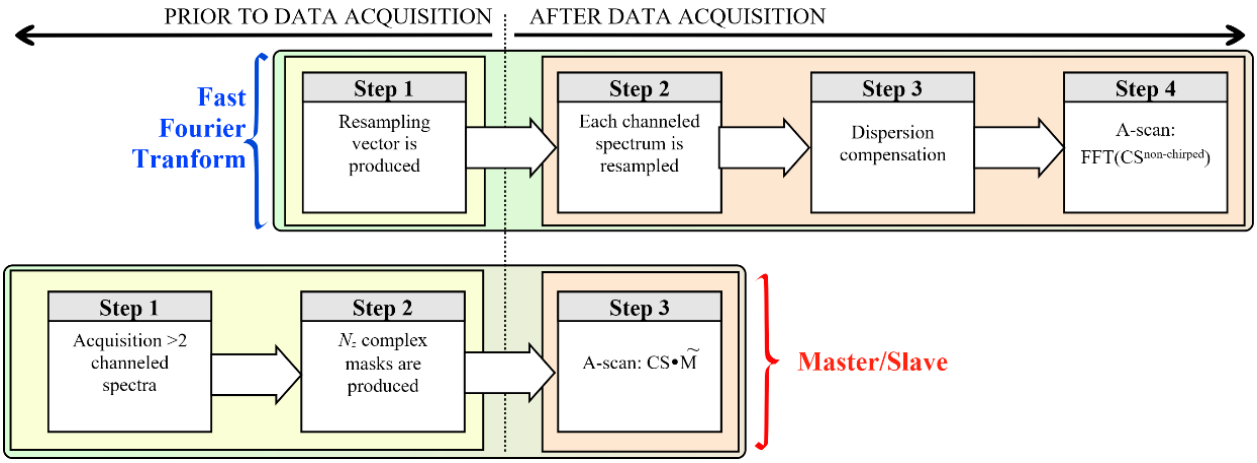

Figure 1. Procedure steps required to produce an A-scan profile using the FT based OCT (top) and to produce a single reflectivity value using the MS method (bottom).

In Fig. 2, the time to produce a B-scan image using the 2 methods as a function of the number of points N_k each spectrum is digitized into is shown.

For the FFT case, a fixed number of points in each A-scan ($N_z=N_k/2$) covers the whole axial range. In opposition, MS has the capability to produce any number of points in the A-scan which cover any axial range.

Two situations are considered for the MS case, $N_z=N_k/2$, to mimic the axial size of the B-scan obtained in FFT based OCT and $N_z=N_k/4$. For the case of resampled FFT method (Res-FFT) (solid circles), data were resampled before FFT.

The FFT requires $N_xN_k\log_2N_k$ operations. When using the MS method, for the same number of $N_z = N_k/2$ axial points, a number of $N_xN_k(2N_k-1)$ operations are required. Therefore, the time to produce a B-scan using FFT is shorter than the time to produce a MS B-scan image (diamonds). Fortunately, high performance toolboxes that take advantage of the multicore design of the CPUs can be used so that the time performance of multiplying matrices (operation required by the MS method) can be tremendously improved (triangles).

For our particular case, (benchmarking performed using a LabVIEW 2015 (National Instruments, Austin Texas) project run on a computer equipped with an Intel I7-5960X @ 3.0 GHz octacore processor (2 logical cores per physical core) and 16 GB of RAM), when $N_k < 5120$, MS produces B-scans faster than the Res-FFT.

Obviously, if data needed to be additionally compensated for dispersion, the FFT based method would have required even longer. Typically, if the emphasis is not on a long axial range, there is no need for a high number of sampling points when digitizing data. For $N_k = 4096$ sampling points, with $N_z = 2048$, a B-scan can be produced in about 102 ms. This does not allow B-scans to be produced during the time of the next frame when using a 50-Hz galvo-scanner. However, such a performance is faster than the Res-FFT (120 ms) but insufficiently quick to categorize the operation as real-time.

An exquisite capability of the MS method is the possibility to reduce the time to display the image by reducing the number of depth points, N_z which is not connected to N_k. The drawback of this operation is either a reduction of the axial range or a less axial resolution. This limitation is not essential in most applications. In our case, although it is possible to achieve an axial range as long as 12.4 mm, in practice this may not be as useful, as very often the axial range is limited by the extension of the confocal gate determined by the scan lens. With squares, we show in Fig. 1 that for a reduced number $N_z = N_k/4$ of axial points in the A-scan the MS technique can provide B-scans faster than its FFTR counterpart for any N_k. When $N_k = 4096$, and $N_z = N_k/4$, a B-scan image can be produced in 52 ms. This however is still insufficient to ensure real-time operation. Further benchmarking (not presented here) showed that for a 50-Hz galvo-scanner, real-time operation can be achieved when $N_z = N_k /10 = 409$, which corresponds to an axial range of around 2.4 mm if the density of masks is kept constant.

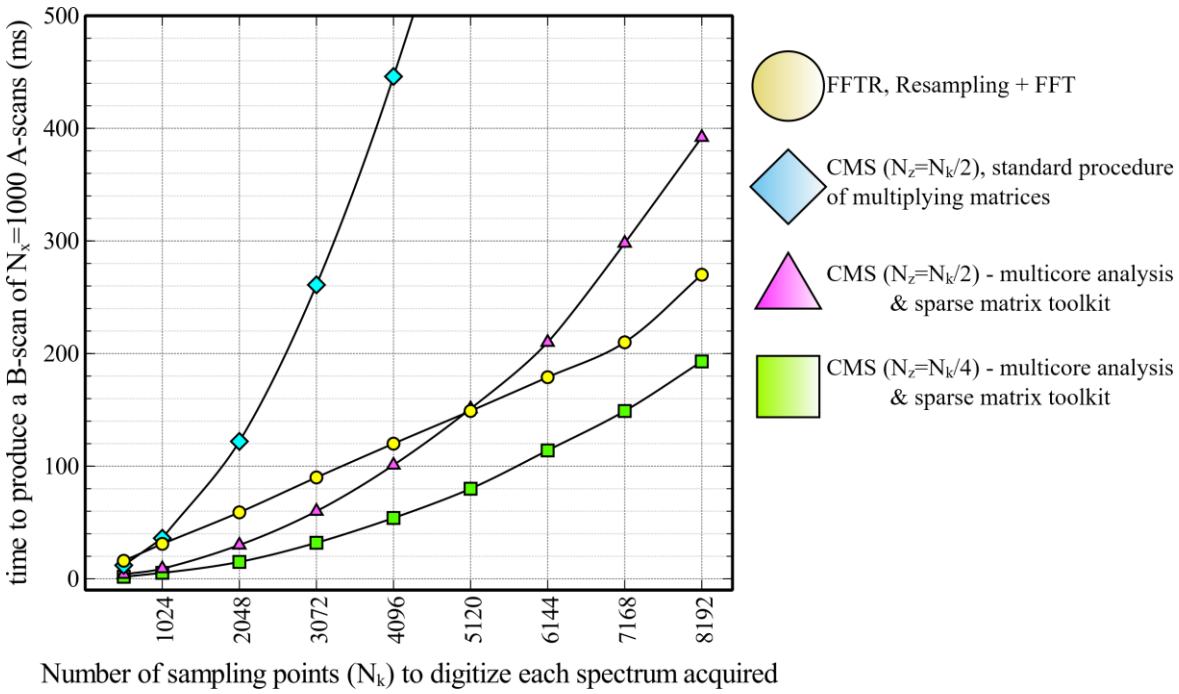

Figure 2. Time to produce a cross-sectional image (B-scan) using both methods, FFT and MS vs the number of sampling points used to digitize each channeled spectrum. Each B-scan is built from N_x=1000 A-scans

3. IMAGING OF THE EYE'S ANTERIOR CHAMBER

Figure 3 shows two images of a volunteer's ocular anterior segment. Both images were produced for the revival order +1, with maximum sensitivity set at δz = 6 mm. Each image, obtained by averaging five adjacent frames was obtained by keeping the length of the reference arm constant and moving the eye axially with respect to the scan lens. In this way, the effect of confocal gate on limiting the axial range is visible. Although our full axial range is around 12.4 mm with little decay in sensitivity from δz_{min} = 0 to δz_{max} = 12.4 mm, depending on the axial position of the eye, different parts of the anterior chamber are brightened up. The coherence revival images exhibit the property that the maximum sensitivity is in the middle of the image (and of the axial range), in comparison with conventional OCT images, where the maximum sensitivity is closer to zero optical path difference.

In Fig. 3(a) the middle of the image coincides with the anterior chamber. In Fig. 3(b), the crystalline lens is closer to the middle of the axial range. Therefore, if in Fig. 3(a) the crystalline lens is hardly visible, it becomes a lot brighter in Fig. 3(b) where the corneal stroma is dimmer. The lateral resolution of the images experimentally measured using an USAF resolution test target is 19.7 μm.

To produce Fig. 3, a number of N_z = 2048 masks (axial points) are used, hence a distance between consecutive masks (axial digital resolution) of about 5.85 μm. Laterally, each image comprises N_x = 1000 pixels, hence a lateral digital resolution of 14.5 μm. Both lateral and axial resolutions are measured in air.

According to the benchmarking shown in Fig. 2, for N_k = 4096 and N_z = 2048 a B-scan can be produced in approximately 100 ms, slightly faster than using the FFT based OCT method. Consequently, the images in Fig. 3, covering an axial range of over 12 mm are produced at a frame rate of 10 Hz, however slower than the frame rate for real-time operation (50 Hz).

When imaging the anterior chamber of the adult human eye, there is no need in principle for more than 6 mm axial range to image the entire segment from the corneal epithelium to the crystalline lens. Using the CMS, the axial range can be adjusted dynamically by simply restricting the axial range of the masks employed. In Fig. 4, a B-scan image of the anterior chamber spanning over 6 mm is shown. To produce it, the same number of N_z = N_k /2 = 2048 masks can be used, corresponding to an axial range of 6 mm. This image was extracted from a movie produced at 10 Hz as N_z = 2048.

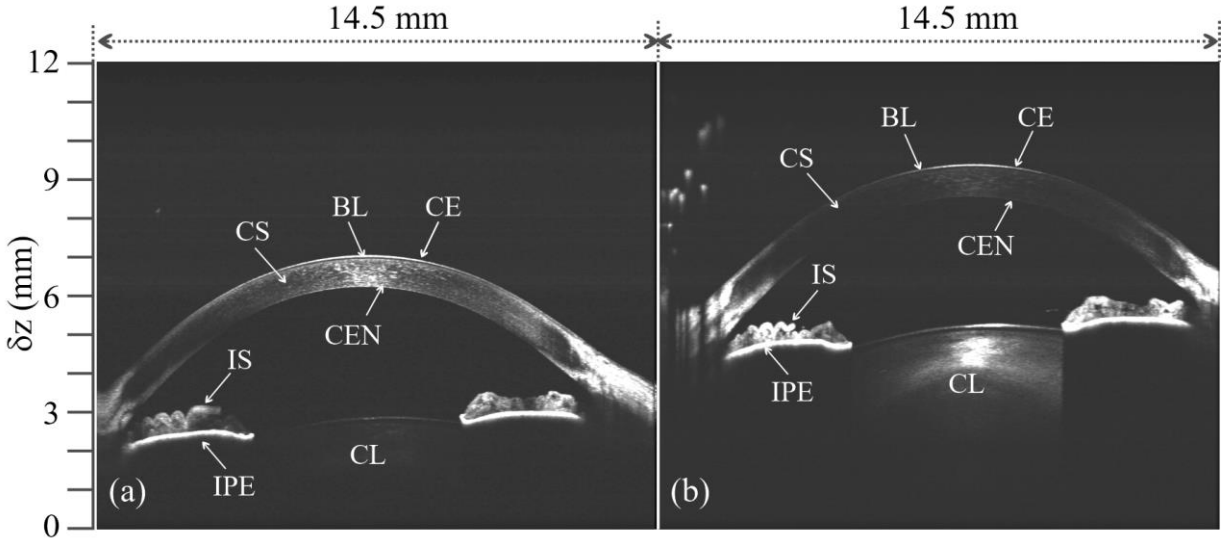

Figure 3. B-scan images of the ocular anterior segment for 2 axial positions of the eye. CE: corneal epithelium, BL: Bowman's layer, CS: corneal stroma, CEN: corneal endothelium, IS: iris stroma, IPE: iris pigment epithelium, CL: crystalline lens.

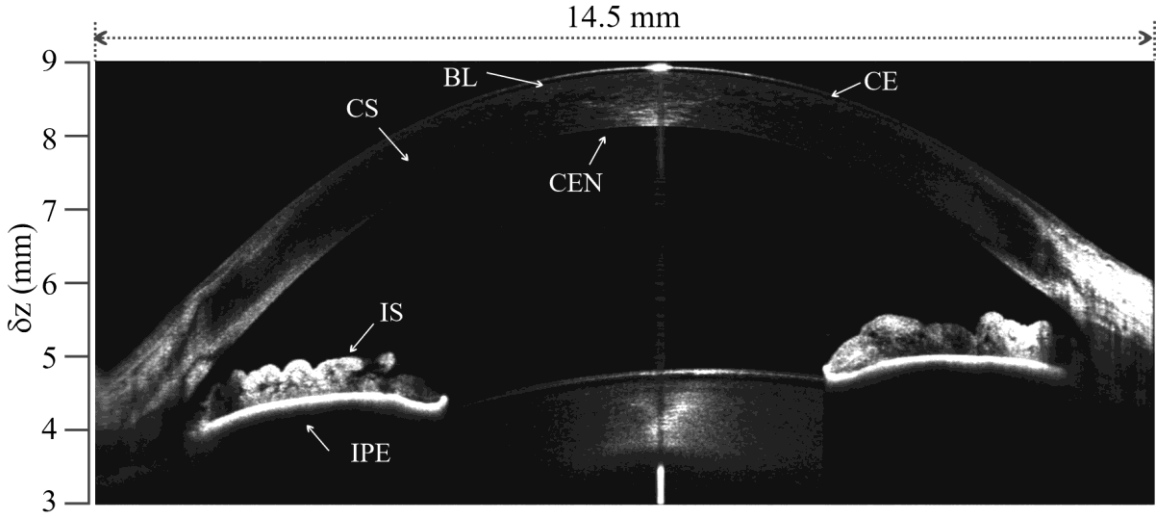

Figure 4. Cross-sectional image of the ocular anterior segment of a healthy volunteer. The image consists of Nx = 1000 pixels laterally and Nz = 2048 pixels axially. CE: corneal epithelium, BL: Bowman's layer, CS: corneal stroma, CEN: corneal endothelium, IS: iris stroma, IPE: iris pigment epithelium, CL: crystalline lens.

For an axial range of 6 mm, the axial distance between two consecutive points, when N_z = 2048 in the A-scans is 2.92 µm, which is much better than the axial optical resolution of the system. To maintain the same digital axial resolution as in Fig. 5, the number of axial points N_z can be halved to 1024, in which case, each frame can be produced at 20 Hz.

As it can be seen in Fig. 5, although axially only N_z = 1024 are used, the axial resolution is preserved, but the speed of producing the images improved by a factor of 2 while still producing mirror free long axial range images over an axial range with little sensitivity drop-off. Fig. 5, is the first frame of a movie (20 Hz frame rate) produced while the laser beam was scanned over the whole anterior chamber.

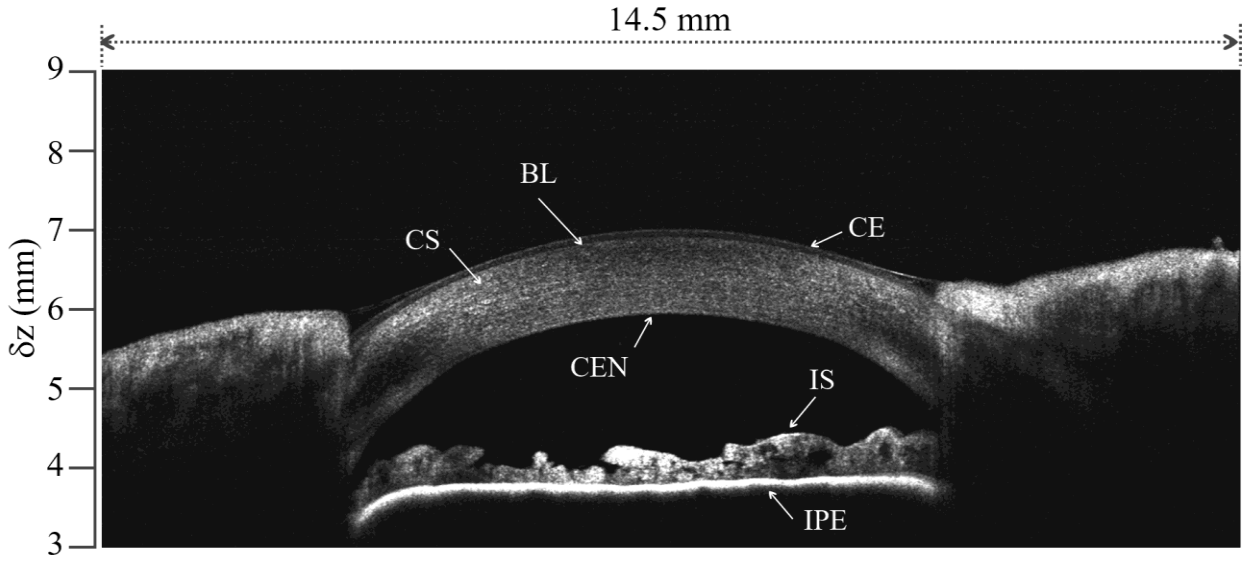

Figure 5. Cross-sectional images of the ocular anterior segment of a healthy volunteer extracted from Visualization 2. The image consists of P = 1000 pixels laterally and R = 1024 pixels axially. CE: corneal epithelium, BL: Bowman's layer, CS: corneal stroma, CEN: corneal endothelium, IS: iris stroma, IPE: iris pigment epithelium, CL: crystalline lens.

4. CONCLUSION

To conclude, the MS-OCT can be an ideal tool for CR-OCT imaging systems. The CR makes the production of long axial range, mirror term free OCT cross-sectional images possible. The MS technique simplifies it even further, as it eliminates the need of data resampling and the need for dispersion compensation, bringing speed to the production of OCT images and lower cost to assembling OCT technology.

When used in conjunction with a coherence revival imaging system, the CMS method can provide images over the same long axial range as its FT based counterpart. However, due to its simpler implementation, CMS has the potential to produce images less affected by artefacts and also faster without resorting to extra hardware equipment.

In MS-OCT, to speed up the production of B-scans, it is possible to act on the size of the axial region of interest to be imaged (ROI). In FT-OCT, this range is determined by the speed of the digitizer that also determines the number of sampling points N_k to digitize each channeled spectrum.

The maximum axial range is determined in both methods, conventional FFT and MS by the number of sampling points N_k used to digitize each channeled spectrum. However, after acquisition, each method offers different functionality in preparing images. In FFT based OCT, the N_k number of points dictates the axial extension of the B-scan OCT image. A smaller region of interest (ROI) is achievable only by cropping the final image. In MS-OCT, the axial ROI is determined by N_z, the number of masks to be used at the Slave stage. Consequently, it is possible to adjust the ROI easily, to match the axial size of the sample to be imaged.

The use of a large number of sampling points N_k for digitization cannot be avoided in a coherence revival system hence an increased computation time to resample data before FFT. MS-OCT solves this issue in an elegant way, by decoupling the axial ROI from N_k. In FFT based OCT, as the optical axial resolution is digitally compromised when an insufficient number of points is used to digitize the channeled spectra, very often data is zero-padded before FFT. In CMS, to tackle this inconvenient, a sufficiently large number N_z of axial reflectivities have to be estimated. For the images shown in the manuscript, we produced axial reflectivities from consecutive points (digital axial resolution) separated by 5.85 μm in Figs. 3 and 5, and 2.92 μm in Fig. 4. Figs. 3 and 5, although showing a lower digital axial resolution, provide either long axial range or speed. As in CMS, the axial ROI can be decoupled from N_k, the number of axial reflectivities N_z can be reduced up to the level where the digital resolution equals the optical one. In FFT based method, due to zero-padding the amount of data produced cannot be limited.

The MS method is an alternative to the FT based method, but better to be combined with the coherence revival technique, as it eliminates several important drawbacks associated to the FFT technique, as no need of zero-padding, re-sampling of data or dispersion compensation is required and allows real-time production of cross-sectional images.

ACKNOWLEDGEMENTS

A. Bradu and A. Podoleanu acknowledge the support of ERC (http://erc.europa.eu) COGATIMABIO 249889. S. Rivet acknowledges the Marie-Curie Intra-European Fellowship for Career Development, No. 625509. A. Podoleanu is also supported by the NIHR Biomedical Research Centre at Moorfields Eye Hospital NHS Foundation Trust and the UCL Institute of Ophthalmology, by the European Industrial Doctorate UBAPHODESA, FP7-PEOPLE-2013-ITN 607627 and by the Royal Society Wolfson Research Merit Award. A Bradu is also supported by the EPSRC – EP/N019229/1.

REFERENCES

[1] Dhalla, A., Nankivil, D. and Izatt, J., "Complex conjugate resolved heterodyne SSOCT using coherence revival," Biomed. Opt. Express 3, 633-649 (2012).
[2] Dhalla, A., Nankivil, D. and Izatt, J., "Complex conjugate resolved heterodyne swept source optical coherence tomography using coherence revival," Biomed. Opt. Express 3(3), 633-649 (2012).
[3] Dhalla, A., Nankivil, D., Bustamante, T., Kuo, A. and Izatt, J., "Simultaneous swept source optical coherence tomography of the anterior segment and retina using coherence revival," Opt. Lett. 37(11), 1883-1885 (2012).
[4] Dhalla, A., Shia, K., and Izatt, J., "Efficient sweep buffering in swept source optical coherence tomography using a fast optical switch," Biomed. Opt. Express 3(12), 3054-3066 (2012).
[5] Bradu, A., Rivet, S., and Podoleanu, A., "Master/slave interferometry – ideal tool for coherence revival swept source optical coherence tomography," Biomed. Opt. Express 7, 2453-2468 (2016).
[6] Rivet, S., Maria, M., Bradu, A., T., Leick, L., and Podoleanu, A., "Complex master slave interferometry," Opt. Express 24, 2885-2904 (2016).
[7] Podoleanu, A., and Bradu, A., "Master–slave interferometry for parallel spectral domain interferometry sensing and versatile 3D optical coherence tomography," Opt. Express 21, 19324-19338 (2013).
[8] Bradu, A., Kapinchev, K., Barnes, F., and Podoleanu, A., "On the possibility of producing true real-time retinal cross-sectional images using a graphics processing unit enhanced master-slave optical coherence tomography system," J. Biomed. Opt., 20(7), 076008 (2015).
[9] Bradu, A., Kapinchev, K., Barnes, F., and Podoleanu, A., "Master slave en-face OCT/SLO," Biomed. Opt. Express 6, 3655-3669 (2015).
[10] Bradu, A., and Podoleanu, A., "Calibration-free B-scan images produced by master/slave optical coherence tomography," Opt. Lett. 39, 450-453 (2014).